PHYSICAL REVIEW B VOLUME 28, NUMBER 12 15 DECEMBER 1983

Lattice dynamics of $SnSe_2$

J.-Y. Harbec
Département de Physique, Université de Sherbrooke, Sherbrooke, Québec J1K 2R1, Canada

B. M. Powell
Chalk River Nuclear Laboratories, Atomic Energy of Canada Limited, Chalk River, Ontario K0J 1J0, Canada

S. Jandl
Département de Physique, Université de Sherbrooke, Sherbrooke, Québec J1K 2R1, Canada
(Received 17 June 1983)

Neutron inelastic scattering measurements of the phonon dispersion curves of $SnSe_2$ have been analyzed in terms of an extended shell model including static dipoles and van der Waals forces between anions. The model provides a good fit to the experimental dispersion curves. Inclusion of the static dipoles is essential to understand the anisotropy of the LO-TO splittings of the infrared-active modes at Γ and the Se ions are found to have a static dipole of $-0.67\ e\ \text{Å}$. The inclusion of van der Waals forces is necessary to fit correctly the LA mode at the zone-boundary point A. The layer character of $SnSe_2$ is exemplified by the weak Se-Se short-range interlayer interaction.

I. INTRODUCTION

Crystals with the CdI_2 structure form a particularly interesting class of binary compounds, for they show the anisotropic properties characteristic of layer compounds while having simple chemical and crystal structures. Many dihalide and dichalcogenide compounds crystallize in this structure.[1] The simplicity of the structure has encouraged several attempts to develop detailed force models for the lattice dynamics of the transition-metal dihalides[2–5] and also of the dichalcogenide $TiSe_2$.[6] In the present paper we employ an extended shell model to describe the dynamics of the dichalcogenide $SnSe_2$. This model is physically more realistic than those applied to date for most other layer structure dichalcogenides [MoS_2 (Ref. 7), $NbSe_2$ (Ref. 8), $TaSe_2$ (Ref. 8)] or monochalcogenides [ϵ-GaSe (Ref. 9) and GaS (Refs. 10 and 11)].

The semiconducting layer compound $SnSe_2$ crystallizes in the CdI_2 structure (space group D^3_{3d}) with one molecule of $SnSe_2$ in the hexagonal unit cell (Fig. 1). Each "layer" perpendicular to the c axis is made up from three planes of ions forming a Se-Sn-Se sandwich with the Sn ion in the center of an octahedral cage formed by the Se ions. The stacking sequence along the c axis is thus Sn-Se-Se-Sn and the layer character of the solid arises from weak interlayer interactions, primarily those such as Se(2)-Se(3) in Fig. 1.

The optical frequencies in $SnSe_2$ have been measured by Lucovsky *et al.*[12] and Harbec and Jandl,[13] and so the (anisotropic) LO-TO splittings at Γ are well established. Brebner *et al.*[14] measured the acoustic branches of the dispersion relation in $SnSe_2$ by inelastic neutron scattering methods. These data were analyzed in terms of a rigid layer model and the elastic constants, C_{11}, C_{33}, and C_{44} were derived from them. These authors also presented a group-theoretical analysis of the lattice vibrations at the major symmetry points of the Brillouin zone. However, they did not include the factor $\exp[-i\vec{G}\cdot(\vec{R}_\kappa-\vec{R}_a)]$ in the transformation matrices,[15] where $\vec{G}$ is a reciprocal-lattice vector, $\vec{R}_\kappa$ is the position of atom κ in the unit cell, and

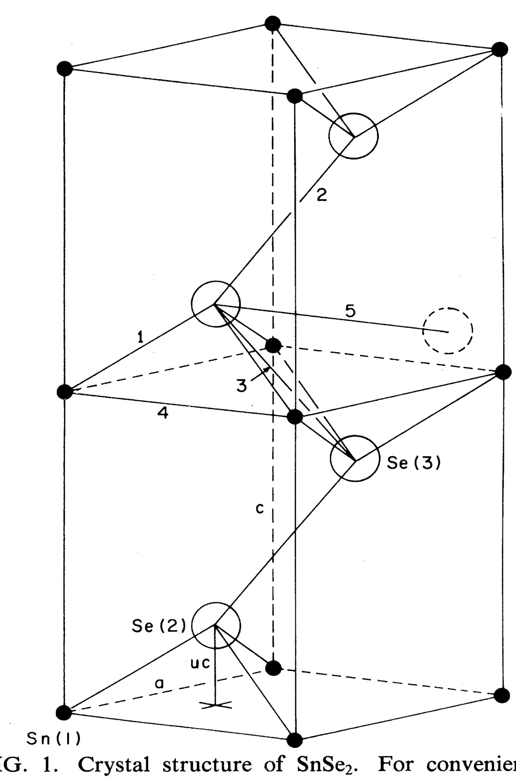

FIG. 1. Crystal structure of $SnSe_2$. For convenience, two unit cells are represented in the figure. The cell parameters are a and c, and the positions of the atoms are, with respect to the hexagonal axes, (0,0,0) for the Sn(1) atom and $(\frac{2}{3},\frac{1}{3},uc)$ and $(\frac{1}{3},\frac{2}{3},(1-u)c)$ for the Se(2) and Se(3) atoms respectively. Numbers 1–5 denote the bonds considered in the model.

$\vec{R}_a$ is the fractional translation associated with the rotation $[a]$. Consequently, certain phase factors for the Se displacements at the zone boundaries are absent.

In this paper we report further inelastic neutron scattering measurements on $SnSe_2$ which extend the previous measurements of the acoustic branches and outline several optical branches of the dispersion relation. The experimental lattice vibration frequencies are then analyzed in terms of an extended shell model (ESM), which also includes contributions from static dipoles and from van der Waals forces.

II. EXPERIMENTAL DETAILS

The two single crystals of $SnSe_2$ used in the experiment were cut from an ingot grown by the Bridgman technique. The specimens, which had a total volume of ≈ 0.8 cm^3, were oriented with the Δ and T directions in the scattering plane and the frequencies of selected phonons were measured at 300 K by the technique of coherent inelastic neutron scattering. The measurements were made on triple-axis crystal spectrometers operated in the constant momentum transfer mode at the NRU reactor, Chalk River. Two combinations of monochromator and analyzer were utilized: (i) Ge(113) and Ge(113) with a resolution of 0.20 THz and (ii) Ge(113) and Be(002) with resolutions of 0.21 and 0.32 THz. The observed dispersion curves are shown in Fig. 2.

III. ANALYSIS

The experimental lattice vibration frequencies were initially analyzed in terms of a rigid-ion model. However, the observed anisotropy of the LO-TO splittings could not be fitted by this model even with the introduction of anisotropic effective charges.[11] Furthermore, short-range forces to at least sixth-nearest neighbors were found to be necessary, but their parameters were physically unreasonable. As a result of these difficulties we did not proceed further with the rigid-ion model but instead chose to analyze the data in terms of a more physically realistic force model, the extended shell model described by Benedek and Frey.[5] This model includes, in addition to the effects of the dynamic dipoles of the ordinary shell model, contributions due to static dipoles present on the selenium ions. The polarizable selenium ions are not on centers of inversion symmetry and thus can be polarized towards the nearest tin ions. In terms of the shell model,

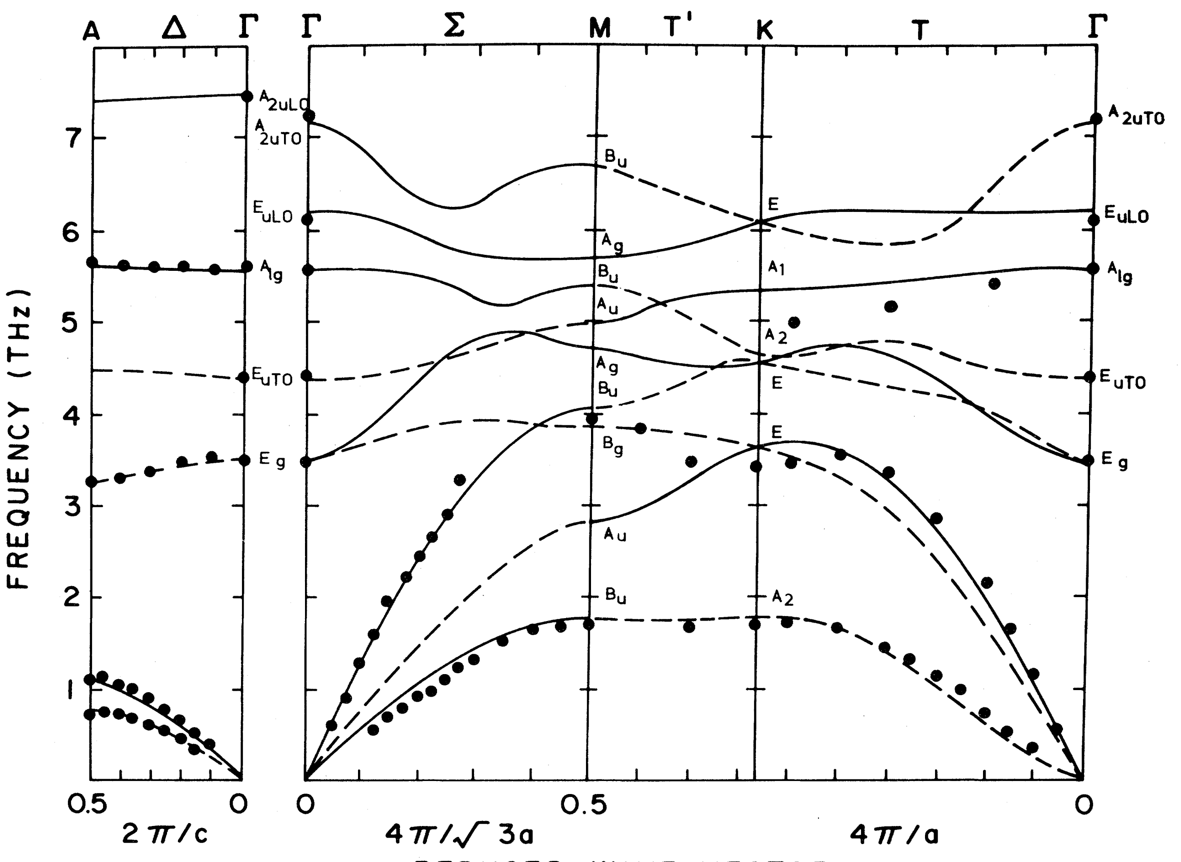

FIG. 2. Phonon-dispersion relations of $SnSe_2$. Solid circles show the experimental measurements, and the lines show the calculations using the shell model with static dipoles. The irreducible representations at A are identical to those at Γ. Solid lines refer to modes with no transverse component parallel to the plane of the layers; for the Δ, Σ, and $T(T')$ directions these are A_1, A', and A modes, respectively. The branches designated by dashed lines refer to the corresponding E, A'', and B modes, respectively.

the static dipoles are created by displacing the center of the mass of the negatively charged Se shells towards the nearest tin ions while the cores are held at their equilibrium positions. This implies that the dynamical matrix must be evaluated for specific relative displacements of the cores and shells. The core-core Coulomb matrices $\underline{C}^{cc}$ can be computed from the static crystal structure, but the core-shell and shell-shell matrices $\underline{C}^{cs}$ and $\underline{C}^{ss}$ have to be computed for each value of the core-shell displacement $\vec{w}_0$. The dipolar forces thus introduced are directly responsible for the anisotropy of the LO-TO splittings.[4,5]

Another contribution, that of the van der Waals forces between selenium ions, is included in the model. These forces are relatively weak and their contribution is only a minor part of the cohesive energy of an ionic solid, but they are important to get a good fit for the acoustic branches along the Δ direction.[5] In our model, the van der Waals forces are considered to act between cores only.

The dynamical equations of the extended shell model are

$$\underline{M}\omega^2(\vec{q})\vec{u}(\vec{q})=\underline{A}(\vec{q})\vec{u}(\vec{q})+\underline{B}(\vec{q})\vec{w}(\vec{q}) , \tag{1a}$$

$$0=\underline{B}^{\dagger}(\vec{q})\vec{u}(\vec{q})+\underline{D}(\vec{q})\vec{w}(\vec{q}) , \tag{1b}$$

where $\vec{u}$ and $\vec{w}$ are the core and shell displacement vectors, respectively, $\underline{M}$ is the mass matrix, ω is the phonon angular frequency, $\vec{q}$ is the wave vector, and $\underline{A}$, $\underline{B}$, and $\underline{D}$ are matrices which include short- and long-range contributions[2]:

$$\underline{A}=\underline{R}^{\mathrm{ASM}}+\underline{R}^{\mathrm{vdW}}+2\underline{G}-\underline{\hat{G}}-\underline{\hat{G}}^{\dagger}+\underline{X}\,\underline{C}^{cc}\underline{X}+\underline{X}\,\underline{C}^{cs}\underline{Y}+\underline{Y}(\underline{C}^{cs})^{\dagger}\underline{X}+\underline{Y}\,\underline{C}^{ss}\underline{Y} , \tag{2a}$$

$$\underline{B}=\underline{R}^{\mathrm{ASM}}+\underline{G}-\underline{\hat{G}}+\underline{X}\,\underline{C}^{cs}\underline{Y}+\underline{Y}\,\underline{C}^{ss}\underline{Y} , \tag{2b}$$

$$\underline{D}=\underline{R}^{\mathrm{ASM}}+\underline{G}+\underline{Y}\,\underline{C}^{ss}\underline{Y} . \tag{2c}$$

The short-range forces are assumed to be axially symmetric and are represented by conventional bond-stretching (A_i) and bond-bending (B_i) force constants.[16] The five shortest bonds in the crystal were included in the model and are listed in Table I. Their contribution is denoted by $\underline{R}^{\mathrm{ASM}}$. The contribution of the van der Waals forces is $\underline{R}^{\mathrm{vdW}}$ and $\underline{X}$ and $\underline{Y}$ are the diagonal core and shell charge matrices, respectively. The definitions of the Coulomb matrices are given by Venkataraman, Feldkamp, and Sahni.[17] The elements of the matrices $\underline{A}$, etc., are denoted by $A_{\alpha\beta}(\vec{q}_{kk'})$, etc., where $\alpha,\beta=x,y,z$ are Cartesian indices (the c axis is along the z direction), and $k,k'=1,2,3$ denote the atoms of the unit cell. Furthermore, if K_k is the force constant between the core of the atom k and its own shell,

$$G_{\alpha\beta}(\vec{q}_{kk'})=\delta_{\alpha\beta}\delta_{kk'}K_k , \tag{3a}$$

$$\hat{G}_{\alpha\beta}(\vec{q}_{kk'})=\delta_{\alpha\beta}\delta_{kk'}K_k[\exp(i\vec{q}\cdot\vec{w}_{0(k)})] . \tag{3b}$$

In our model, the core and shell of the tin ion are considered as rigidly coupled, so that $K_1\to\infty$. The axially symmetric forces act through the shells only, and the actual position of the shells must be taken into account in computing R^{ASM}.

The van der Waals contribution is calculated from the potential[18]

$$E_{kk'}(r)=-\frac{C_{kk'}}{r^6} , \tag{4}$$

where the constant $C_{kk'}$ can be approximated by the London formula:

$$C_{kk'}=\tfrac{3}{2}\alpha_k\alpha_{k'}\frac{E_kE_{k'}}{E_k+E_{k'}} . \tag{5}$$

We consider the interaction to act between selenium atoms only. E_k is then an average excitation energy of the selenium ion, taken as 3.9 eV after Camassel *et al.*,[19] and α_k is the polarizability of the ion, estimated at 7 Å^3 after Tessmann, Kahn, and Shockley.[20] With these values, the constant of the van der Waals interaction is 230×10^{-79} J m^6.

The model thus includes five short-range interactions, the Se core shell force constant K_2, the core and shell charges X_{Se} and Y_{Se}, and the static displacement of the selenium shell w_0. The parameter w_0 determines the Coulomb matrices $\underline{C}^{cs}$ and $\underline{C}^{ss}$. The matrices are used in the fitting procedure, but their evaluation is very time-consuming. Consequently we parametrize them in the form

$$C^{ij}_{\alpha\beta}(\vec{q}_{kk'})=C^{cc}_{\alpha\beta}(\vec{q}_{kk'})+w_0S^{ij}_{\alpha\beta}(\vec{q}_{kk'})+w_0^2T^{ij}_{\alpha\beta}(\vec{q}_{kk'}) , \tag{6}$$

where $\underline{S}$ and $\underline{T}$ are matrices whose elements were computed to reproduce the variation of $\underline{C}^{cs}$ and $\underline{C}^{ss}$ over the range $0<w_0<0.40$ Å. The approximation is excellent within these limits. The model thus has 14 adjustable parameters.

The equilibrium positions of cores and shells are determined by the four parameters a, c, u, and w_0, where a and c are the lattice constants of the hexagonal structure, and uc is the distance between a plane of anions and the nearest plane of metal atoms. For the ideal CdI_2 structure, $c/a=(\frac{8}{3})^{1/2}$ and $u=\frac{1}{4}$. The derivatives of the potential with respect to the parameters a, c, and u give the conditions

$$-\frac{\partial\Phi^C}{\partial a}=a(2B_1+B_2+B_3+3B_4+6B_5) , \tag{7a}$$

$$-\frac{\partial\Phi^C}{\partial c}=c(6u^2B_1+3(1-2u)^2B_2+12u^2B_3) , \tag{7b}$$

$$-\frac{\partial\Phi^C}{\partial u}=c^2(6uB_1-6(1-2u)B_2+12uB_3) . \tag{7c}$$

TABLE I. Description of the short-range bonds in $SnSe_2$. The bond lengths are calculated assuming $u=0.25$.

Bond number	Description	Length (Å)
1	Sn-Se intralayer	2.676
2	Se-Se oblique interlayer	3.769
3	Se-Se oblique intralayer	3.769
4	Sn-Sn horizontal intralayer	3.799
5	Se-Se horizontal intralayer	3.799

TABLE II. Parameters for the shell model with static dipoles. The short-range force constants are in units of N m.$^{-1}$.

$A_1=105.0\pm2.5$		$B_1=1.0\pm0.7$
$A_2=3.5\pm0.9$		$B_2=0.9\pm0.2$
$A_3=37.8\pm4.0$		$B_3=-9.7\pm0.7$
$A_4=4.1\pm2.9$		$B_4=-0.2\pm0.7$
$A_5=20.4\pm3.9$		$B_5=2.0\pm0.7$
	$K_{\text{Se}}=430\pm15$	
$X_{\text{Se}}=(2.16\pm0.04)e$		$Y_{\text{Se}}=(-3.36\pm0.04)e$
$w_0=0.20\pm0.01$ Å		

Since the short-range forces act between shells, the parameter u will not have the value 0.25, but rather $0.25-w_0/c$. The derivatives of the Coulomb potential Φ^C must be evaluated taking into accout the actual positions of cores and shells. For $w_0=0.20$ Å, we find

$$\frac{\partial\Phi^C}{\partial a}=(1.705X^2+5.125XY+3.322Y^2)e^2/a^2\ , \tag{8a}$$

$$\frac{\partial\Phi^C}{\partial c}=(2.736X^2+4.765XY+2.076Y^2)e^2/a^2\ , \tag{8b}$$

$$\frac{\partial\Phi^C}{\partial u}=(17.593X^2+33.172XY+15.600Y^2)e^2/a\ , \tag{8c}$$

where X and Y denote the charges on the Se ion. The equilibrium condition arising from the parameter w_0 is much more complex and can only be solved by an iterative procedure.[5] This condition was not used in the fitting process. The first three equilibrium conditions were imposed during the initial iterations of the fitting but were later relaxed to obtain the "best-fit" parameters.

The dispersion curves calculated using the best-fit parameters are shown in Fig. 2 and the parameters are given in Table II. The model provides a fair description (quality of fit $\chi=3.7$) of the observed dispersion curves. The zone-center frequencies and the anisotropy of the acoustic branches are well reproduced. This anisotropy is reflected in the Se-Se interlayer force constant (A_2), which is 30 times smaller than A_1. The Se-Se oblique intralayer constant A_3 is unexpectedly strong, though repulsive ($B_3<0$), while the Se-Se horizontal intralayer constant A_5 is attractive. The values for B_1 and B_2 given in Table II agree with the corresponding values calculated from the equilibrium conditions, but the best-fit value for B_4 (-0.2 ± 0.7 N m^{-1}) is in significant disagreement with that calculated from equilibrium (-12.4 ± 2.3 N m^{-1}).

An analysis of the different contributions to the model[5] shows that the static dipoles are the dominant contribution to the anisotropy of the LO-TO splittings. In our model, the Se ions carry a charge of $-1.2e$ and have a static dipole of $-0.67\ e$ Å. The last result is in reasonable agreement with the value $-0.83\ e$ Å calculated by van der Valk and Haas,[21] but these authors find an effective charge of $-0.48e$. In the present model, no combination of X_{Se}, Y_{Se}, and w_0 can reproduce the LO-TO splittings for such a small charge transfer. However, the static dipoles alone are not responsible for the anisotropy of the LO-TO splittings, inclusion of the electronic polarizability simulated by the shell model is also essential. Introducing static dipoles in a rigid-ion model will not cause anisotropic LO-TO splittings, although they will produce some anisotropy between the A_{2u} and E_u modes that otherwise would be absent.

The contribution of the van der Waals forces to the dynamical matrix is in general relatively small. Typically, it accounts for 2—6% of a given matrix element. The phonon frequency most strongly affected by the van der Waals forces is that of the A_{2u}(LA) mode at the A point, which would be 35% higher without the van der Waals contribution. Models which do not taken into account the van der Waals forces[2,3] yield unphysically low charge transfer in order to reproduce the acoustic branches along Δ.

IV. SUMMARY

The ESM model gives fair agreement between the experimental and fitted dispersion curves. The electronic polarizability and the static dipoles included in the model account for the anisotropic LO-TO splittings satisfactorily, which suggests that a model of *at least* this complexity is necessary to describe adequately the dynamics of this dichalcogenide. The layer character of $SnSe_2$ is shown by the weak Se-Se interlayer interaction, whose parameters are determined principally by the acoustic branches along Δ. The ratio A_1/A_2 for $SnSe_2$ is 30, at the high end of the range exhibited[2-5,9-11] by other layer compounds (15—30).

[1]R. W. G. Wyckoff, *Crystal Structures*, 2nd ed. (Interscience, New York, 1963), Vol. 1.
[2]A. Pasternak, J. Phys. C 9, 2987 (1976).
[3]A. Pasternak, Solid State Commun. 26, 685 (1978).
[4]A. Frey and R. Zeyher, Solid State Commun. 28, 435 (1978).
[5]G. Benedek and A. Frey, Phys. Rev. B 21, 2482 (1980).
[6]Y. Yakaoka and K. Motizuki, J. Phys. Soc. Jpn. 49, 1838 (1980).
[7]N. Wakabayashi, H. G. Smith, and R. M. Nicklow, Phys. Rev. B 12, 659 (1975).
[8]D. E. Moncton, J. D. Axe, and F. J. DiSalvo, Phys. Rev. B 16, 801 (1977).
[9]S. Jandl, J. L. Brebner, and B. M. Powell, Phys. Rev. B 13, 686 (1976).
[10]B. M. Powell, S. Jandl, J. L. Brebner and F. Lévy, J. Phys. C 10, 3039 (1977).
[11]A. Polian, K. Kunc, R. Le Toullec, and B. Dorner, in *Physics of Semiconductors, 1978,* edited by B. L. H. Wilson (IOP, London, 1979), p. 907.
[12]G. Lucovsky, J. C. Mikkelsen, W. Y. Lian, R. M. White, and R. M. Martin, Phys. Rev. B 14, 1663 (1976).
[13]J.-Y. Harbec and S. Jandl, Phys. Rev. B 25, 6126 (1981).
[14]J. L. Brebner, S. Jandl, and B. M. Powell, Nuovo Cimento 38B, 263 (1977).
[15]S. H. Chen, Phys. Rev. 163, 532 (1967).
[16]G. W. Lehman, T. Wolfram, and R. E. DeWames, Phys. Rev. 128, 1593 (1962).
[17]G. Venkataraman, L. A. Feldkamp, and V. C. Sahni, *Dynam-*

ics of Perfect Crystals (MIT Press, Cambridge, 1975), p. 243 and Appendix 2.

[18]M. P. Tosi, in *Solid State Physics,* edited by F. Seitz and D. Turnbull (Academic, New York, 1964), Vol. 16, p. 29.

[19]J. Camassel, M. Schlüter, S. Kohn, J. P. Voitchovsky, Y. R. Shen, and M. L. Cohen, Phys. Status Solidi B 75, 303 (1976).

[20]J. R. Tessmann, A. Kahn, and W. Shockley, Phys. Rev. 92, 890 (1953).

[21]H. J. L. van der Valk and C. Hass, Phys. Status Solidi B 80, 321 (1977).